

Development of Statistical Bridge Signatures for Structural Health Monitoring

A thesis submitted by

Christopher W. Follen

In partial fulfillment of the requirements

for the degree of

Master of Science

in

Civil and Environmental Engineering

Tufts University

August 2013

Co-Advisors: Brian Brenner, P.E. & Masoud Sanayei, Ph.D.

Abstract

An instrumentation system was implemented on the Powder Mill Bridge in Barre, Massachusetts. The instrumentation was designed as a research prototype for development of a structural health monitoring system. Strain data from permanently installed strain gauges was collected for truck events over a period of six months. Maximum strain values from heavy truck events were used to establish statistical distributions which describe behavior of the undamaged bridge under normal operating conditions. Prediction intervals were added to the statistical distributions. A calibrated finite element model of the bridge was used to simulate damage scenarios, including large scale and localized damage of the bridge deck. Analytical distributions of a damaged bridge model were plotted against experimental distributions of the undamaged bridge with prediction intervals. It was shown that, given 1500 future heavy truck events, all three damage scenarios studied would be detectable.

Certificate of Fitness

Acknowledgments

First, I would like to thank the National Science Foundation and the Federal Highway Administration, as the funding for this research was provided by NSF-PFI Grant No. 0650258, and by FHWA LTBP Program (Federal Contract Number DTFH61-08-00005, Sub-award Number 00004397).

I would like to thank MassDOT and the Town of Barre for access to the Powder Mill Bridge on Vernon Avenue, and for their continued support of this project. Thanks to Fay Spofford & Thorndike Inc. for sharing with us the design drawings and calculations. Thanks to Geocomp Corporation for providing and assisting with the installation of the onsite data acquisition system, and for continued technical support.

Thanks to John Phelps, for allowing me to use his calibrated finite element model of the Power Mill Bridge.

I would like to thank my co-advisors Brian Brenner and Masoud Sanayei for their continued support and feedback on my project. Thanks to Rich Vogel, for all of his contributions to this research, and for agreeing to be a part of this project despite the fact the he was on sabbatical during much of this process.

I am extremely grateful to have had the pleasure of working with doctoral candidate Jesse Sipple, who provided me with substantial support and guidance. Jesse was always willing to help, and consistently provided me with valuable input.

I would like to thank my fellow graduate students: Anish Kayiparambil Pushpangadan, Alex Reiff, Tianqi Qu, Paul Rosenstrauch, Merve Iplikcioglu, and Ali Khaloo – It has been a pleasure working with all of you.

I would like to thank my parents for instilling in me the desire to work hard, and to realize my own potential. Thanks to my father especially, for his continued support of my education.

Finally, I would like to extend a most sincere thank you to my girlfriend Katie, who has provided me with unwavering support throughout this process. Without her, this would not have been possible.

Table of Contents

Abstract.....	ii
Certificate of Fitness	iii
Acknowledgments.....	iv
Table of Contents	vi
List of Figures	viii
List of Tables	ix
1. Introduction	1
2. Statistical Bridge Signatures.....	2
2.1 Abstract.....	2
2.2 Introduction	3
2.3 Powder Mill Bridge.....	7
2.4 Long-Term Monitoring System	9
2.5 Definition and Development of a Bridge Signature	11
2.6 Nonparametric Prediction Intervals for Bridge Signatures.....	14
2.7 Sample Size Needed for Stable Bridge Signatures	13
2.8 The Use of a Bridge Signature for Damage Detection	18
2.9 Implementation of Proposed Damage Detection System	23
2.10 Conclusions	24
3. Powder Mill Bridge.....	28
3.1 Site and History.....	28
3.2 New Powder Mill Bridge	29
3.3 Instrumentation of Powder Mill Bridge	32
3.4 Data Acquisition System at Powder Mill Bridge	36
4. Long-term Truck Event Data Collection System.....	41
4.1 Collection of Truck Events at PMB	41
4.2 Automated Collection of Strain Data via iSiteCC Program.....	41
4.3 Trigger Program	41
4.4 Additional Long-term Strain Collection Programs	45
5. Powder Mill Bridge Calibrated Finite Element Model	46

5.1	Background on Powder Mill Bridge Calibrated Finite Element Model	46
5.2	Undamaged and Damaged Model Truck Runs	46
6.	Conclusions	49
6.1	Overall Conclusions	49
6.2	Future Work	50
Appendix A: Powder Mill Bridge Supplemental Information.....		52

List of Figures

Figure 2-1. Powder Mill Bridge.....	7
Figure 2-2. On Site Data Acquisition System.....	8
Figure 2-3. Powder Mill Bridge Sensor Layout.....	9
Figure 2-4. Strain Output from Example Powder Mill Bridge Truck Event	10
Figure 2-5. Histograms of Maximum Strain Outputs from Captured Truck Events	10
Figure 2-6. Histograms of Maximum Strain Outputs from Heavy Events.....	11
Figure 2-7. Bridge Signatures or Survival Distribution Functions of Maximum Strain Outputs from Heavy Truck Events on Powder Mill Bridge.....	13
Figure 2-8. SDF Values vs. Number of Events Included for SG+	14
Figure 2-9. Bootstrapped SDF Data Sets.....	16
Figure 2-10. Prediction Intervals Overlaid on Bootstrapped Data Sets.....	18
Figure 2-11. Damage Cases 1 and 2, Analytical SDF's due to Large Scale Deck Damage.....	21
Figure 2-12. Damage Case 3 Analytical SDF's due to Localized Deck Damage	24
Figure 3-1. Powder Mill Bridge Location.....	28
Figure 3-2. Old Powder Mill Bridge.....	29
Figure 3-3. Plan View of Powder Mill Bridge.....	30
Figure 3-4. Typical Cross Section of Powder Mill Bridge	31
Figure 3-5. PMB Sensor Station Locations	33
Figure 3-6. Installed Strain Gauge on Powder Mill Bridge.....	36
Figure 3-7. PMB DAQ System Architecture Schematic	38
Figure 3-8. UPS Installed onsite	39
Figure 3-9. New Laptop Installed Onsite.....	40
Figure 4-1. Locations of 18 Selected Strain Gauges.....	43

List of Tables

Table 3-1. PMB Sensor Inventory	32
Table 3-2. PMB Instrumentation Schedule, Stations 0 – 6.....	34
Table 3-3. PMB Instrumentation Schedule, Stations 7 – 12.....	35
Table 3-4. PMB iSite Box Information.....	37
Table 5-1. Absolute Maximum Strains from Calibrated Finite Element Model	47
Table A-1. Sensor Information for 18 Selected Strain Gauges on PMB	52
Table A-2. Data Acquisition System Information for 18 Selected Strain Gauges	53

1. Introduction

This thesis is divided into six main chapters and one appendix. The purpose of this first chapter is to provide detailed information on the structure of the thesis. Chapter 2 is a manuscript on development and for use of statistical bridge signatures, and is formatted for future publication. Chapter 3 provides background information on the Powder Mill Bridge, and the prototype structural health monitoring system that has been installed on site. Chapter 4 details the system that I installed and configured on site to automatically and continuously collect strain data from truck events on the bridge. Chapter 5 discusses my use of a calibrated finite element model of the Powder Mill Bridge in validation of the proposed structural damage detection system. Chapter 6 discusses conclusions drawn from this research, and areas that should be studied further.

Due to the fact that Chapter 2 is a stand-alone manuscript, references for each chapter is included at the end of the corresponding chapter.

2. Statistical Bridge Signatures

2.1 Abstract

Instrumentation of bridge structures provides a stream of data representing operational structural response under loading. We define the term, “bridge signature”, as the expected response of a particular bridge under loading, as measured by different instruments. In this research, we propose a new a new method to develop and evaluate a bridge signature. The signature can be monitored over time and statistically evaluated to detect potential structural deterioration and damage.

An instrumentation system was implemented on the Powder Mill Bridge in Barre, Massachusetts as a research prototype for development of a structural health monitoring system. Heavy truck events due to daily traffic are collected using an automatic measurement system which triggers above a given threshold of recorded strains. Using the measured strain data due to daily traffic, a bridge signature is created using nonparametric statistical techniques. Maximum experimental strain values from heavy truck events were used to establish a nonparametric probability distribution which describes the behavior of the undamaged bridge under normal operating conditions. Nonparametric prediction intervals are added to the bridge signature, which define where future distributions of strain data from the undamaged bridge should fall.

In order to study the robustness of this method for use in damage detection, three damage scenarios are created using a calibrated finite element model. Comparison of the prediction intervals of the undamaged bridge signature with the analytical damaged distributions show that for all three damage scenarios, the damaged distributions fall outside of those intervals, which indicates that this method can potentially identify the presence of structural damage. This study

shows that the proposed method is robust and computationally efficient for operational bridge damage detection using only measured strain data from truck loadings.

Keywords: Structural health monitoring, SHM, strain measurements, long-term monitoring, damage detection, Bootstrap method, reliability, prediction intervals, nonparametric

2.2 Introduction

Traffic volumes in the United States have increased from 1.81 trillion miles traveled annually in 1986, to 2.98 trillion miles in 2011 (FHWA, 2011). The Federal Highway Administration estimates that by the year 2050, Americans will travel approximately five trillion vehicle miles annually (USDOT, 2010). This increase in traffic volume has taken a toll on our nation's infrastructure. Of the 605,000 bridges in the US, some 67,000 are classified as structurally deficient and more than 76,000 are labeled functionally obsolete (FHWA, 2012). The increase in American dependence on infrastructure and the deteriorating state of the nation's bridges, coupled with high construction costs and limited funding illustrates the need to improve efficiency and reduce costs associated with bridge management and maintenance.

Currently in the United States, bridges are inspected at least once every two years (FHWA, 2004). Bridge inspections are performed using methods that haven't changed much in decades. Bridges are manually inspected, mostly relying upon visual observations. In some cases, additional non-destructive tests may be specified, but the majority of the work is by visual inspection. After inspection, the engineer prepares a report on the bridge's condition. This process is to an extent, subjective, and different engineers may rate the same bridge differently. Given that these bridge reports help guide maintenance decisions of the bridge owners, a more objective inspection system is desirable.

Developing technology offers new opportunities for bridge inspection and resulting decisions for maintenance. Finite element modeling and structural health monitoring (SHM) of bridges can provide bridge owners with a more objective evaluation of a bridge's performance and structural health, and can potentially reduce maintenance costs and increase public safety.

Doebbling et al. (1996) provides a literature review of SHM and damage detection techniques, and Farrar and Worden (2007) offers an introduction to SHM which includes a discussion of the history of SHM techniques, motivation for systems, and system implementation considerations.

Sartor et al. (1999) discussed the economic advantage of SHM systems, noting that short-term monitoring of structures can provide significant insight into structural behavior and help bridge owners determine whether or not structural rehabilitation is necessary.

Olund and DeWolf (2007) described a long-term structural health monitoring project in which a combination of strain measurements, rotations, accelerations, and temperatures were taken on three bridges in Connecticut over the course of several years. Alampalli and Lund (2006) presented a methodology for estimating fatigue life of certain bridge components through collection and processing of strain data.

Cardini and DeWolf (2008) installed a system to collect truck event strain data from a steel girder highway bridge over time. The authors discussed the possibilities of using a change in load distribution factors to each girder, peak strain range, or neutral axis location as a sign of structural damage. Orcesi and Frangopol (2010) presented a methodology for including long-term truck event strain measurements in bridge serviceability analysis by calculation and use of moment distribution factors for bridge girders.

While it is relatively straightforward to predict bridge outputs (e.g. static strains or dynamic accelerations) given bridge inputs (e.g. truck size, load path, and weight distribution, or dynamic excitation locations and frequency range), the loading inputs are not always easily obtained. In some cases load tests have been performed with a truck of known size and weight, and strain output data has been collected and correlated. At best, load tests can only be performed occasionally, and in the case of many highway bridges, closing the structure for testing, even occasionally, is unrealistic due to impacts on traffic. These constraints make it desirable to develop an automated system of structural health monitoring and damage identification that is based on bridge data collected under operational conditions.

Ni et al. (2008) presented a system for identifying structural damage on a cable-stayed bridge using mode shapes, but noted that in some cases structural damage can be masked by ambient factors such as temperature change or traffic pattern variations. Scianna and Christenson (2009) proposed a method in which random traffic excitation data was used to excite the bridge health monitoring benchmark problem. Their method used change in natural frequencies to identify structural damage, and included a probabilistic framework for dealing with the variation in excitation due to traffic variability. The method did not, however, account for changing environmental conditions such as temperature variation or wind loading.

Catbas et al. (2012) presented the possibility of using video imaging to record vehicles crossing a bridge and to classify the vehicles using a database of known vehicle types for comparison. Such a system could help estimate the axle spacing of vehicles, and even provide approximate weight distributions. However, this method needs refinement, and may not be able to predict weight distributions accurately enough to identify damage based on changes in strain readings.

We propose a new method of structural damage identification for bridges, through the establishment of a “bridge signature”, and the addition of prediction intervals. The signature is defined as an expected response of a bridge structural system to daily traffic as measured by an instrumentation system. This response can be evaluated by nonparametric statistical methods which employ a very limited number of assumptions and enable the development of prediction intervals associated with the signature. Our approach documents how the bridge signature can be defined over a period of time. Variations from the baseline prediction intervals associated with the bridge signature may indicate structural damage.

We have collected truck loading events (that is, when a truck crosses the bridge) for approximately six months. The strain data from these events was used to estimate a nonparametric cumulative probability distribution of maximum strain outputs that we define to be the bridge signature. We assert that any change in this signature over time may be indicative of changes in structural element properties here referred to as “structural damage”. We show that given certain damage scenarios, our nonparametric statistical approach can identify the presence of structural damage, using only strain outputs from future monitoring, and without any information about the loading inputs.

This approach for bridge structural health monitoring is unique because it decouples the measured structural response from detailed finite element analysis. Using high quality measurements at strategic locations on the bridge, it is possible to match bridge measured responses with a perfectly precise structural analysis. Then, any variation of measurements from the model over time would suggest specific structural damage. However, errors in measurement and modeling make a precise match difficult to achieve. By using a nonparametric statistical approach instead, the errors are decoupled from the problem, to an extent.

2.3 Powder Mill Bridge

The new Powder Mill Bridge carries Vernon Avenue over the Ware River (Figure 1). It replaced an older, deteriorated structure and was opened for traffic in September 2009. The bridge is located in Barre, Massachusetts, and is owned by the Town of Barre. It is a three-span continuous steel girder composite concrete deck slab bridge with two lanes running north-south across the river. This bridge was selected because it is a typical bridge that is frequently used in the US highway system.



Figure 2-1. Powder Mill Bridge

The main span is 23.5 meters (77.1 feet) in length, while Span 1 and Span 3 are 11.75 meters (38.6 feet). The bridge was instrumented with a variety of sensors, including 100 strain gauges (Figure 2).



Figure 2-2. On Site Data Acquisition System

The Powder Mill Bridge is near the town of Barre's waste management station. Although the site is rural, large trucks frequently cross the bridge travelling to and from MA Route 122. This ideal location provides a steady stream of loading events on the bridge which in turn have helped supply the data for this research.

Instrumentation was completed in October 2009. Sanayei et al. (2012) provided a complete description of the Powder Mill Bridge and its instrumentation. Figure 3 shows the bridge instrumentation layout. For this study, the authors will focus on outputs from two strain gauges: SG-34 and SG-42. SG-34 is located on Girder 3 near the South Pier measuring strains due to negative moments; SG-42 is located on Girder 3 near the center of the main span measuring strains due to positive moments. These specific gauges were chosen as they are near the center of the roadway on the lower flange of the steel girder, and SG-34 is located roughly in the location that will receive the maximum negative bending stress, while SG-42 is located in the area that will receive the maximum positive bending stress. From this point forward, for the sake of readability, SG-34 and SG-42 will be referred to as SG- and SG+, respectively.

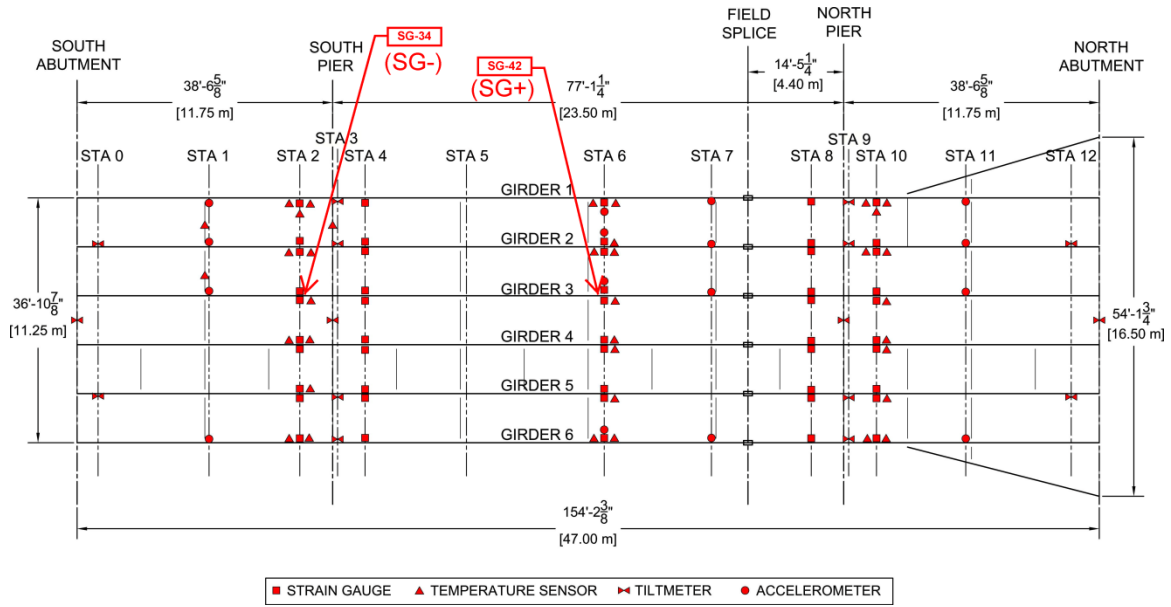


Figure 2-3. Powder Mill Bridge Sensor Layout

2.4 Long-Term Monitoring System

We developed a long-term monitoring program to collect measured strain data from truck events. This system was deployed onsite in July 2012. Since July 2012 we have collected strain data from truck events at a sampling rate of 50Hz (0.02 second intervals). Our program is currently set up to collect strain data for vehicles weighing more than approximately 36 kN (8.1 kips). The program identifies a truck event, and then zeroes the strain readings based on the ambient strain in each sensor prior to the event. Strain readings are “zeroed” by recording only the changes in strain due to the event. Absolute strain values due to temperature changes or residual strains due to construction included in the event data are not recorded. Note that the processing and saving of the truck events is done by an onsite computer, which can be remotely accessed to allow for downloading of the truck event data. Figure 4 shows strain outputs from a typical truck

event on the Powder Mill Bridge. Note that in Figure 4, for clarity, a moving average filter was used in plotting the strain outputs to eliminate the small dynamic effects.

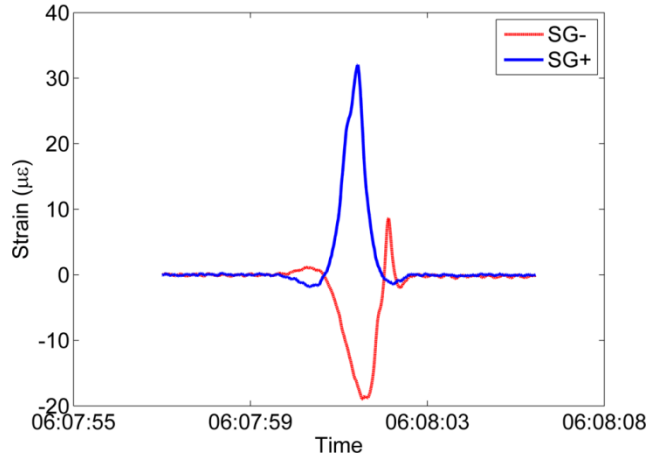


Figure 2-4. Strain Output from Example Powder Mill Bridge Truck Event

We collected strain data from truck events for 88 days spaced intermittently between July 2012 and January 2013. In total we collected strain data from 5,135 truck events. Figure 5 shows the histograms of the absolute maximum strain output per event. These histograms illustrate the bimodal nature of the probability distribution of the truck event strain output.

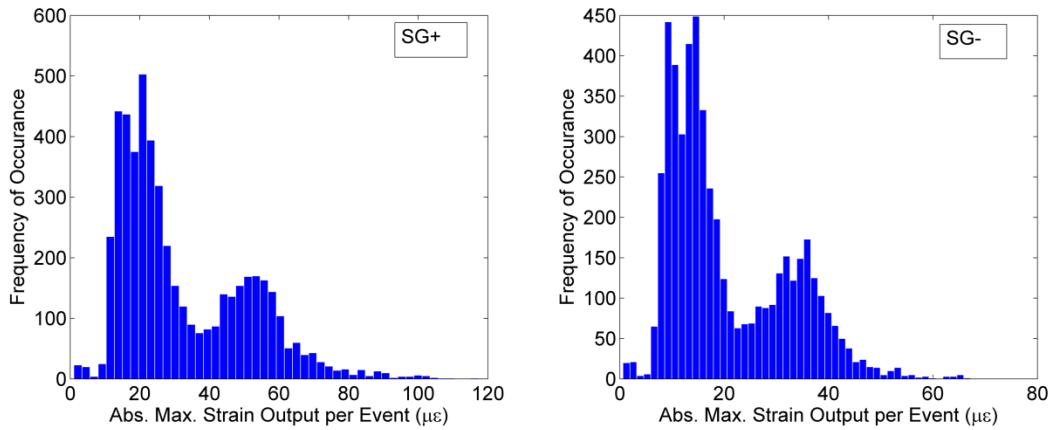


Figure 2-5. Histograms of Maximum Strain Outputs from Captured Truck Events

Based on the histogram of SG+ maximum values in Figure 5, we defined a “heavy truck event” as an event from which the maximum strain output from SG+ was greater than $39\mu\epsilon$ that is equivalent to a live load stress level of 7.79 MPa (1.13 ksi). On the upper end these strains were as large as about $110\mu\epsilon$ that is equivalent to a live load stress level of 22.0 MPa (3.19 ksi). This strain value was selected for this bridge and data set due to its bimodal histogram. This was done to simplify the histogram for modeling of heavier trucks that potentially can observe changes in the bridge superstructure. This strain threshold resulted in a total of 1,670 measured heavy truck events. Figure 6 shows the histograms of the absolute maximum strain values from SG+ and SG-, from the same heavy truck events.

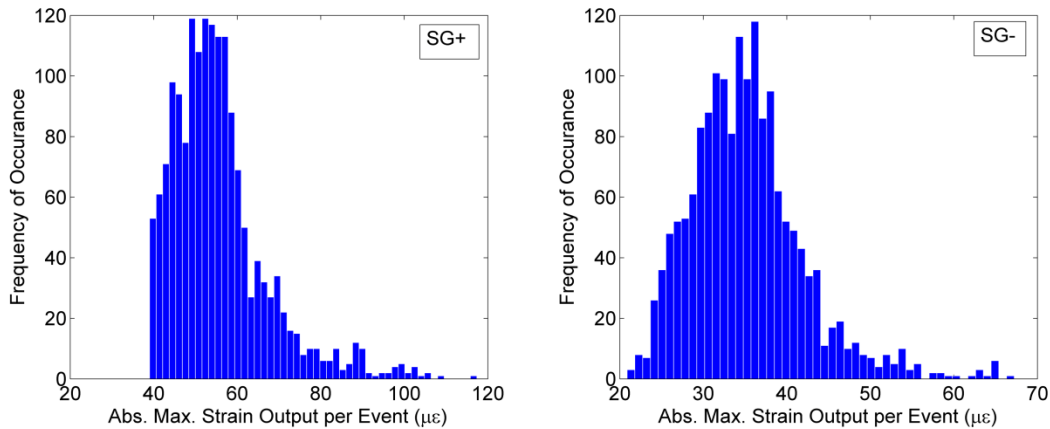


Figure 2-6. Histograms of Maximum Strain Outputs from Heavy Events

2.5 Definition and Development of a Bridge Signature

The histograms illustrated in Figure 6 represent the probability density function (PDF) of absolute maximum strain output, normally defined using the function $f(\epsilon)$, where ϵ is the strain. The characteristic shape of each PDF defines the bridge signature. Comparisons among probability distributions using various goodness-of-fit statistics and hypothesis tests are usually

performed using the cumulative distribution function (CDF), $F(\varepsilon)$, or its complement $(1 - F(\varepsilon))$, which is termed the survival distribution function (SDF). For example, standard hypothesis tests (e.g. Chi-Square test, Kolmogorov-Smirnov test, etc.) which are used to distinguish between PDF's or CDF's (or equivalently between SDF's) are normally based on the CDF or its inverse quantile function (NIST, 2012). All such distributional goodness-of-fit approaches involve comparisons between theoretical probability distribution functions and data such as shown in Figure 6. The proposed approach here is nonparametric, avoiding the need to identify a theoretical PDF or CDF. For a more complete review of nonparametric approaches to the estimation of CDF's and SDF's, refer to (Vogel and Fennessey, 1994). For each of our two critical strain gauges, for n heavy truck events and $i = 1, \dots, n$, the absolute maximum strain values per event, $\varepsilon_{(i)}$, are ranked such that $\varepsilon_{(1)}$ is the largest observed value and $\varepsilon_{(n)}$ is the smallest. The proposed signature SDF's are defined as the ordered values of the absolute maximum strain output per heavy truck events plotted against their probability of exceedance, p_i , using a Weibull plotting position $p_i = i / (n+1)$ where i is the rank of the observation and n is the sample size. A plotting position is simply an estimate of the exceedance or non-exceedance probability of the observation of rank i . The Weibull plotting position is attractive because it provides an unbiased estimate of the exceedance probability regardless of the PDF or CDF from which the strain measurements originate (David, 1981). Alternatively, and equivalently, the SDF curves can be estimated using

$$E_p = \varepsilon_{(i)} \quad \text{if } i = [(n + 1)p]$$

$$E_p = \varepsilon_{(i+1)} \quad \text{if } i < [(n + 1)p]$$

where the quantity in brackets $[(n + 1)p]$ denotes the integer component of the quantity $(n+1)p$ that will always be less than or equal to $(n+1)p$. Note that more complex and accurate nonparametric estimators of the SDF are possible as shown by Vogel and Fennessey (1994), however such estimators are only needed for when sample sizes are generally quite small (i.e. $n < 50$). The simple estimator above uses the rank associated with each observation to obtain its exceedance probability. More advanced estimators outlined in Vogel and Fennessey (1994) involve two or more ranks, along with their associated observations to obtain resulting SDF curves for each value of exceedance probability p . E_p is then plotted versus p to create the SDFs, as shown in Figure 7, for SG+ and SG-.

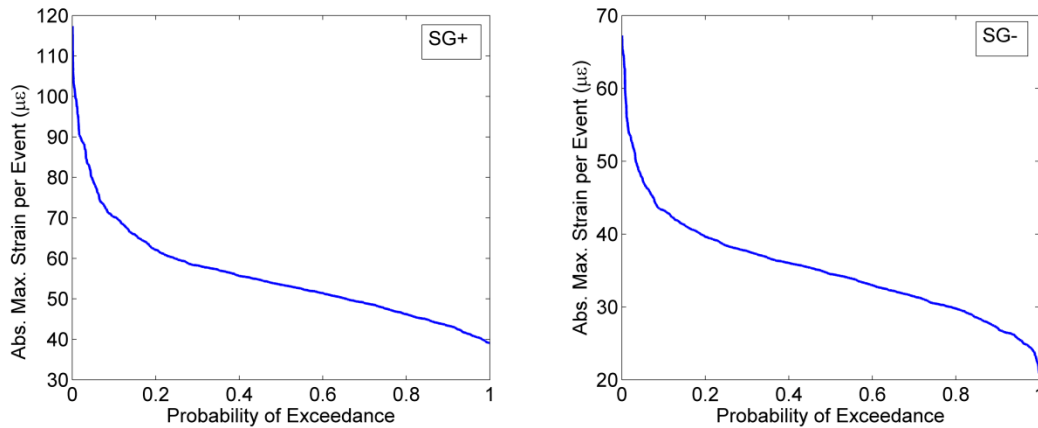


Figure 2-7. Bridge Signatures or Survival Distribution Functions of Maximum Strain Outputs from Heavy Truck Events on Powder Mill Bridge

2.6 Sample Size Needed for Stable Statistical Bridge Signatures

Here we address the question of how many heavy truck events are needed to provide a stable and reproducible statistical bridge signature or SDF. A small collection (on the order of 5 to 50) of

heavy truck events is not enough to capture the variability in traffic loading, or to give a good sense of the distribution of maximum strain outputs over the long-term. A stable SDF would be a curve in which the strain value at a certain probability of exceedance does not change significantly when more data from the same distribution (i.e. that of the undamaged bridge) is added. Figure 8 illustrates the signature SDF value from SG+ at different percentiles versus the number of heavy events used to develop the signature. It illustrates that a stable estimate of the SDF is obtained when the number of events exceeds roughly $n=1000$. This result may be unique to this bridge, and future research is needed to ensure that this minimum sample size results in stable SDF's for other bridges.

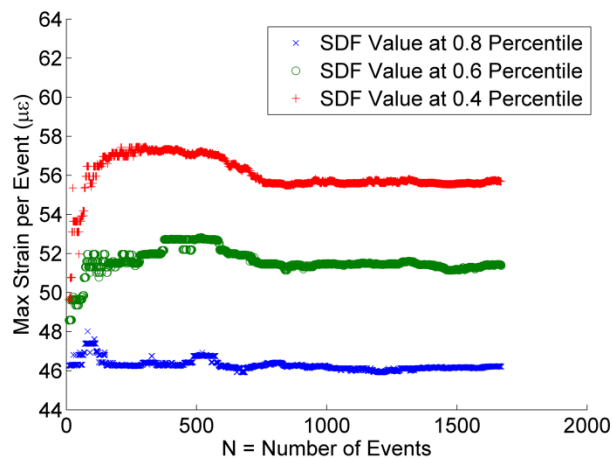


Figure 2-8. SDF Values vs. Number of Events Included for SG+

2.7 Nonparametric Prediction Intervals for Bridge Signatures

A goal is to develop an approach which can reliably distinguish between a bridge signature for a damaged bridge and an undamaged bridge. To distinguish between bridge signatures, it is necessary to understand the variability of estimates of individual bridge signatures or SDF's. Parametric confidence intervals for CDF's or SDF's require assumptions for distribution of data.

However, our approach is nonparametric. Therefore a nonparametric approach is also needed for deriving confidence intervals which do not depend upon any statistical assumptions regarding the underlying probability distribution of the measured strain data. Bootstrapping is a nonparametric statistical resampling method that can be used to evaluate the sampling properties of any statistic including an SDF or CDF. A thorough introduction to Bootstrapping can be found in Efron and Tibshirani (1993). The bootstrap method is a computational approach which replaces complex statistical theory with computer-intensive resampling of the available data. The bootstrap can be used to solve nearly any traditional statistical problem.

Bootstrapping is implemented by sampling randomly with replacement from the observed data set, to create additional data sets which can be used in further statistical analysis. The theory of the bootstrap has shown that for independent and identically distributed random variables, such resampling, with replacement will preserve all the statistical properties of the data, including its SDF and CDF. In our case, the observed data sets are the absolute maximum strain values from the 1,670 heavy truck events from SG- and SG+. For each of the two critical strain gauges, we used the bootstrap to develop two new sets of resampled data. Each new resampled data set was then used to develop 1000 new resampled SDF curves. Figure 9 shows the first resampled data sets obtained via bootstrapping resulting in $n = 200$ events per SDF. The second data sets were constructed via bootstrapping resulting in $n = 1500$ events per SDF in Figure 9.

These SDF's or bridge signatures, derived from bootstrapped data sets show that as the number of heavy truck events per SDF is increased, the variability between the curves decreases. If we assume no damage to the bridge, no significant traffic pattern changes, and no issues with the data acquisition system, the data sets with $n = 200$ can be interpreted as reflecting the behavior of the SDF's or bridge signature that 1000 sets of 200 heavy trucks crossing the bridge (in the

future) could produce; the data sets with $n = 1500$ can be interpreted as the bridge signature or SDF's that 1000 sets of 1500 heavy trucks crossing the bridge could produce in the future.

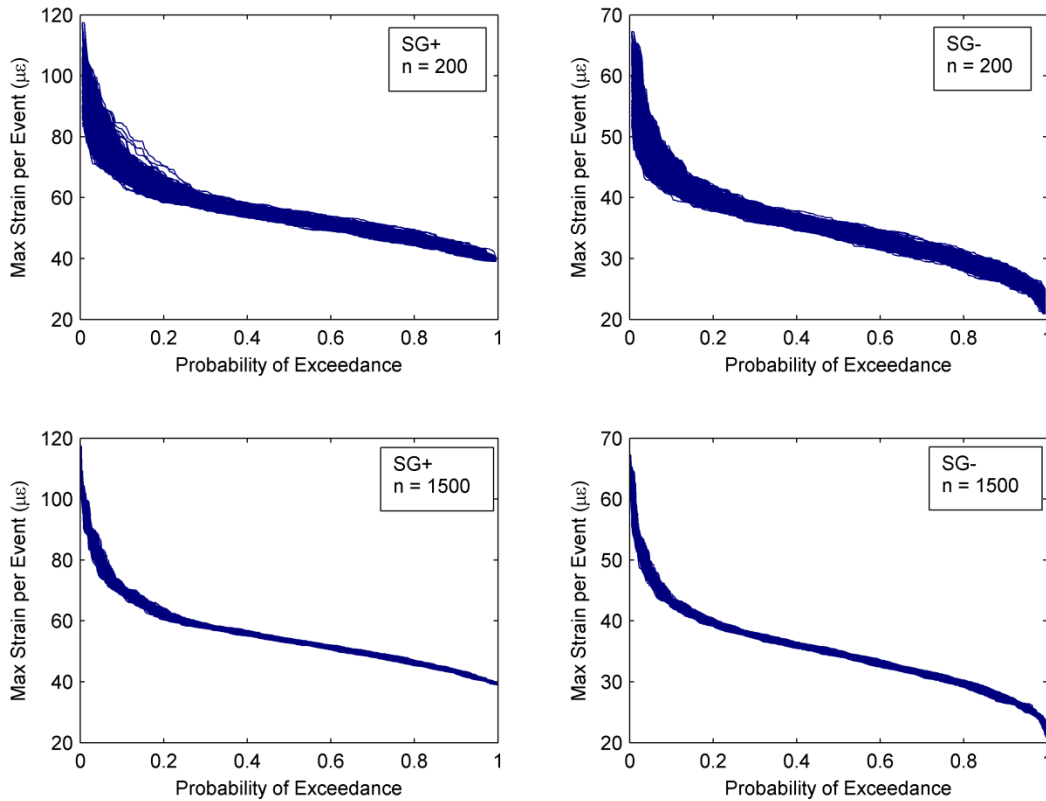


Figure 2-9. Bootstrapped SDF Data Sets

Non parametric prediction intervals can be added to the SDF's in Figure 9 as was suggested originally by Vogel and Fennessey (1994) for hydrologic applications. Each of the 1000 SDF's, or bridge signature curves, or 1000 sets of E_p , is made up of the ordered values $\epsilon_{(i,j)}$ for $i = 1, \dots, n$, as previously defined, and $j = 1, \dots, 1000$. For each i , $\epsilon_{(i,j)}$ can be ranked such that $\epsilon_{(i,1)}$ is the largest and $\epsilon_{(i,1000)}$ is the smallest observation. For 95% prediction intervals with 1000 curves, 5% of the events at each i value should fall outside the intervals, that is, the 95% prediction interval values at each i value are

$$PI_{HIGHER\ BOUND(i)} = \varepsilon_{(i,25)}$$

$$PI_{LOWER\ BOUND(i)} = \varepsilon_{(i,975)}$$

The 95% prediction intervals for each of the four sets of bootstrapped SDF curves are shown in Figure 10 along with the 1000 SDF's used for their creation. The interpretation of the prediction intervals in these figures is critical. We wish to determine the number of loading events that provides sufficient basis for a reliable and reproducible definition of the bridge signature.

Use of data sets with more truck events should lead to prediction intervals closer to one another. More importantly, Figure 10 suggests that excluding significant traffic pattern changes, data acquisition system damage, or structural damage to the bridge, 95% of all future bridge signatures (made up of either 200 or 1500 heavy truck events, as appropriate) should fall within the given prediction intervals. If a future bridge signature collected from the Powder Mill Bridge falls outside the established prediction intervals, that would suggest that traffic patterns changed significantly, the data acquisition system malfunctioned, or that structural damage has occurred. Of these three possibilities, the data acquisition system malfunction in which only the strain values from the sensors increase by moderate amounts is highly unlikely. If significant traffic pattern changes were to occur, it is likely that the shape of a future SDF would change, rather than the entire SDF shifting up or down. Therefore, if the shape of a future SDF curve is consistent with the signature SDF, but the future curve lies wholly or in part outside of the established prediction intervals, it is likely that structural damage has occurred.

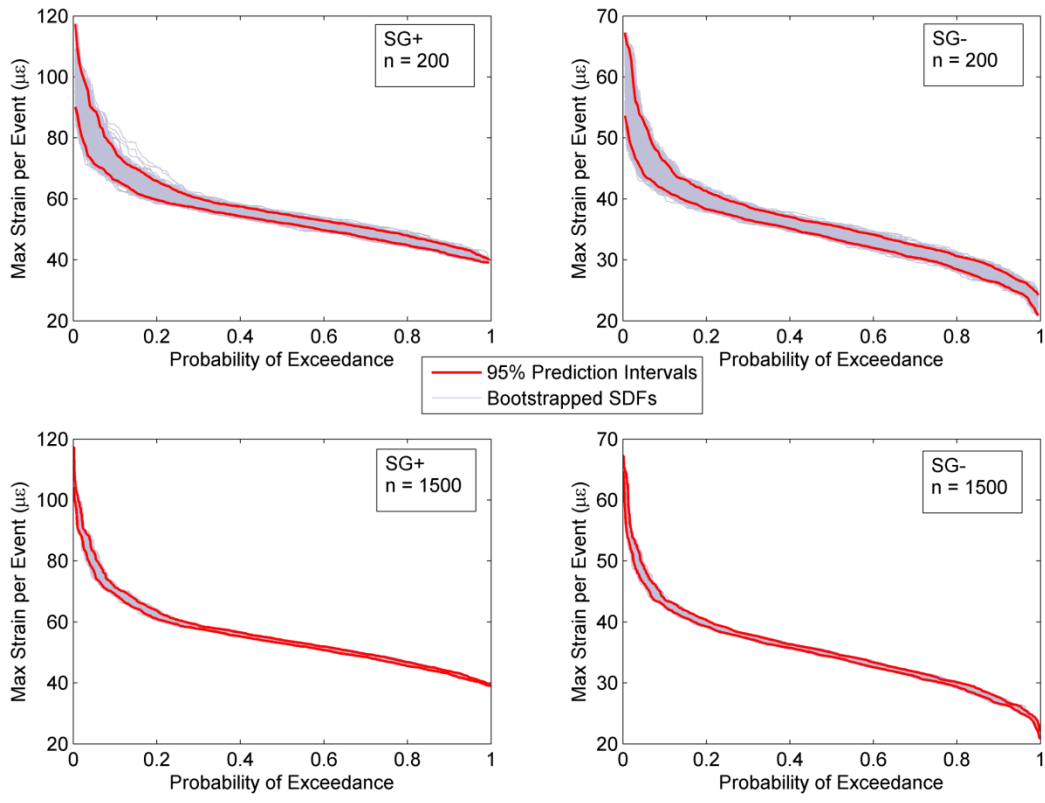


Figure 2-10. Prediction Intervals Overlaid on Bootstrapped Data Sets

2.8 The Use of a Bridge Signature for Damage Detection

The authors used a calibrated finite element model of the Powder Mill Bridge to simulate damage scenarios. For more information on the model and model calibration, refer to Sanayei et al. (2012).

Deck repairs cost bridge owners more than all other maintenance activities combined (Lee, 2012). There are many causes of concrete deck damage which include alkali-silica reaction, reinforcement corrosion, and freezing and thawing. Some damage scenarios would result in a large section of the deck being compromised, while other scenarios, such as rebar delamination

or pot holes might be more localized. For any type of deck deterioration scenario, the bending stiffness of the deck is reduced.

In order to examine the capacity of the proposed method for identification of structural damage, a signature distribution of a damaged bridge must be created for comparison. Given that damaging the actual structure is not feasible, we chose to model damage scenarios using our calibrated finite element model.

Three different damaged scenarios on the Powder Mill Bridge were simulated. Damage Case 1 was a 20% reduction in the bending stiffness of the concrete deck over the entire positive bending region of span 2. Damage Case 2 was a 50% reduction in the bending stiffness of the concrete deck over the entire positive bending region of span 2. Damage Case 3 was a 50% reduction in the bending stiffness of a two-meter by two-meter area in the center of the southbound lane at the midpoint of span 2, representing localized damage.

The Powder Mill Bridge model was calibrated using strain data from a load test, which was performed using a three-axle dump truck. It therefore can be assumed that using the three-axle dump truck statistics for which the model was calibrated, the model will simulate reasonably accurate strain values for linear elastic events.

First, the three-axle dump truck was run over the entire length of the undamaged bridge FE model twice: once on the northbound lane, and once on the southbound lane. The maximum strain values at the locations of SG- and SG+ from each truck run were saved. Next, for each of the three aforementioned damage scenarios, the three-axle dump truck was simulated over the model in the same fashion. For each damage scenario, the percentage change in maximum strain values from the undamaged runs were calculated, and the percent change values from the

northbound run and the southbound run were averaged in each damage case. This processes resulted in estimates of the percentage differences between the maximum strain values (due to the dump truck) of the undamaged case and the three damaged cases. Given linear elastic behavior of the structure, we assume that a damaged bridge signature would be the measured undamaged bridge signature shifted by the percentage change for the appropriate damaged scenario.

Figures 11 and 12 show the damaged analytical SDF's plotted with the experimental SDF's and the previously established prediction intervals. Figure 11 indicate that 20% deck damage in Damage Case 1 on the main span positive bending region could be detected because the bridge signature for the damaged signature of SG- lies outside the 95% prediction intervals for the undamaged bridge signature using 200 new heavy truck events. However, for the same damage scenario, more trucks would be needed for the change to be detectable using only SG+ data. Interestingly, this damage scenario would be detectable using SG+ after collecting about 1500 new heavy trucks. Note that on Figures 11 and 12, the probability of exceedance on the horizontal axis ranges from 0.3 to 0.8 – this is done solely for purposes of plot readability.

Figure 11 also indicates that 50% deck damage in Damage Case 2 on the main span positive bending region could be readily detected by using data from either SG- or SG+, and would require fewer than 200 new heavy truck events.

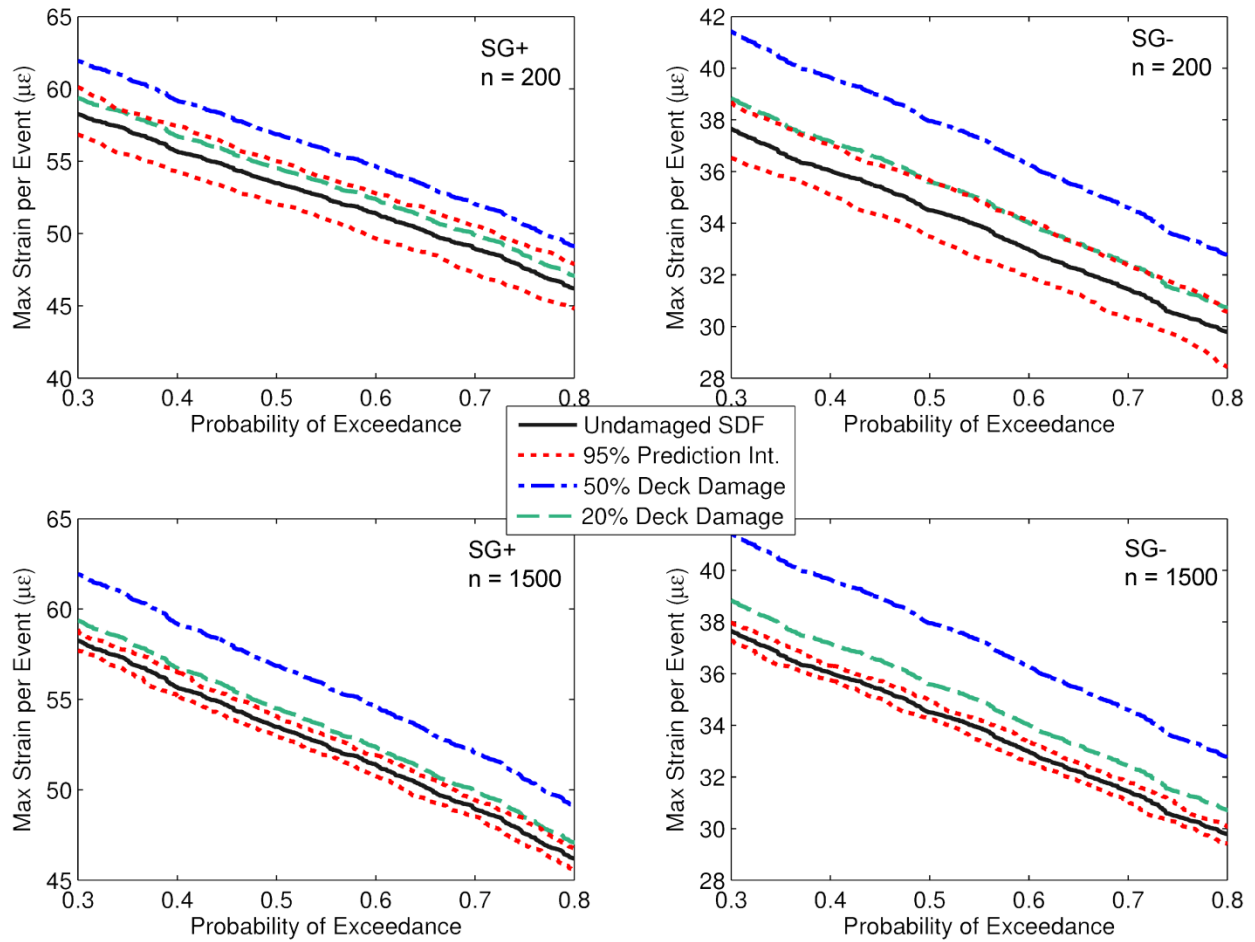


Figure 2-11. Damage Cases 1 and 2, Analytical SDF's due to Large Scale Deck Damage

Figure 12 suggests that the 20% localized deck damage in Damage Case 3 would not be detectable using SG- data, even with 1500 new heavy truck events. This damage scenario could, however, be detected using SG+ data and collecting approximately 1500 new heavy truck events and comparing the new SDF with the undamaged signature SDF.

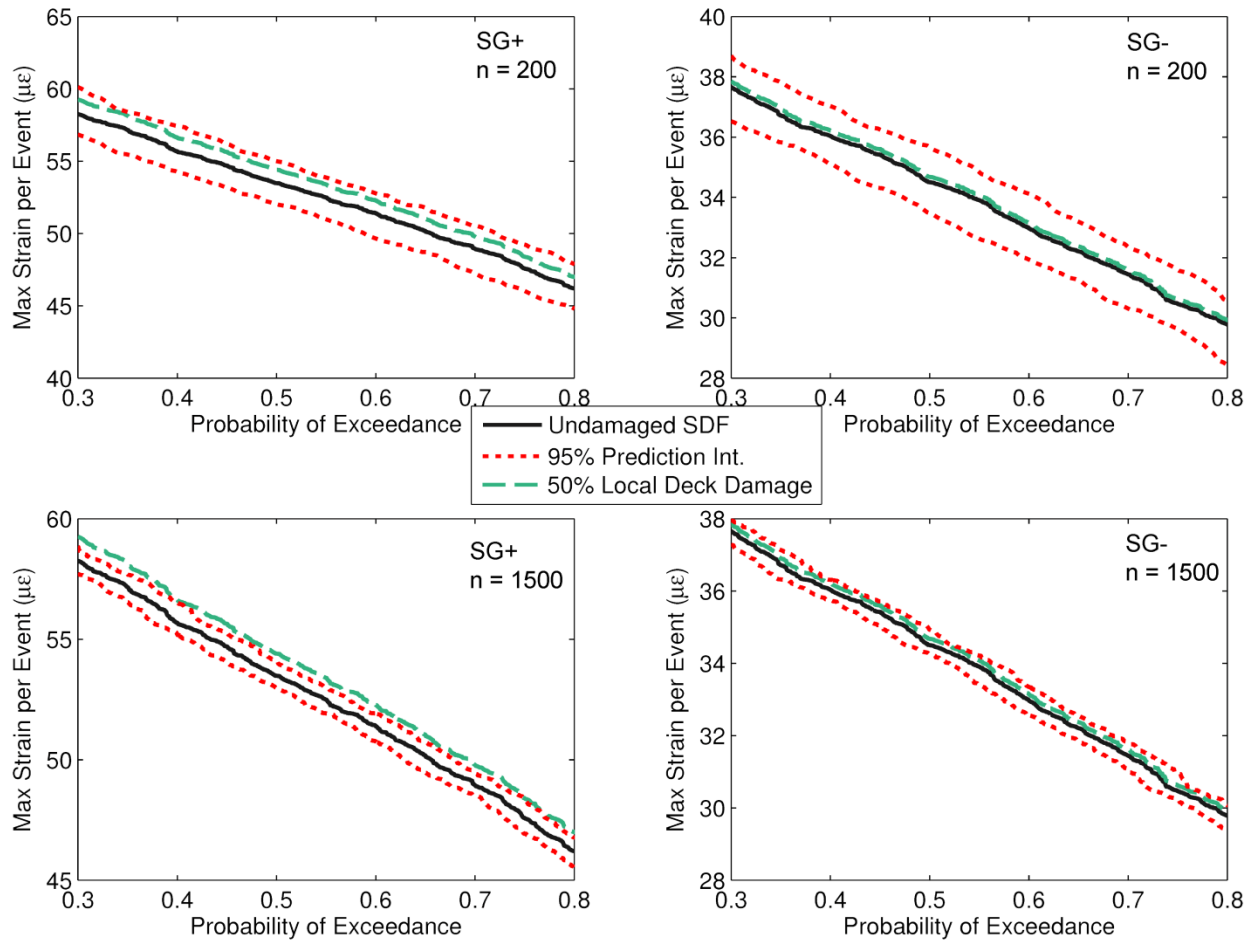


Figure 2-12. Damage Case 3 Analytical SDF's due to Localized Deck Damage

The number of new heavy truck events required to detect a given damage scenario is based on how much of a change the given damage scenario would cause in the maximum strain outputs at SG- or SG+. As more heavy truck events are collected and compared to the signature SDF's, the prediction intervals become smaller. Therefore, the number of new heavy events required to detect a certain damage scenario would be simply a number large enough such that the prediction intervals fall inside of the damaged SDF.

The proposed damage detection method could be implemented as an early warning system for some types of structural bridge damage. Bridge owners could begin measuring strain data (or other types of data) just after the bridge opening, and could establish the signature distribution.

Over the life of the bridge, new distributions could be plotted daily (using perhaps a moving window of, say, 1500 heavy truck events). Each day, the current distributions could be checked against the signature distribution. Additional prediction intervals could be also be added to the signature distribution. Perhaps, both 75% and 95% prediction intervals could be established, and each day the automated system could check to see where the current distribution falls. A new distribution inside the 75% prediction intervals could yield a green light, between the 75% and 95% prediction intervals could yield a yellow light, and outside of the 95% prediction intervals could yield a red light. Bridge owners could greatly benefit from such a simplified and automated system. Note that a ‘green light’ would simply mean that the system has not found any structural changes, and it could not be interpreted as no structural damage is present. The green light /yellow light / red light could be implemented alongside, not in place of, typical visual bridge inspections.

On the Powder Mill Bridge, for this study, we collected strain data for 1,670 heavy truck events over 88 days, which is equivalent to approximately 130 heavy events per week.

2.9 Implementation of Proposed Damage Detection System

We did not have access to a damaged bridge, and therefore we simulated damage on the newly constructed Powder Mill Bridge using a calibrated finite element model. Implementation of this system for damage detection would not require application a calibrated finite element model. Therefore, the success of the approach is not dependent upon resolution of errors associated with FE modeling and matching corresponding bridge response. The proposed system uses only in-situ bridge traffic loading and statistical manipulation of strain outputs to identify damage. The

proposed method is an operational damage detection system, rather than an input/output-based system.

In this study, we focused on strain outputs from two critical strain gauges. For a full scale implementation of this system, more strain gauges could be monitored and included. Analysis could be performed on the outputs of each strain gauge, and findings of each gauge could be synthesized using statistical techniques.

2.10 Conclusions

A new method is proposed and implemented for a long-term structural health monitoring and damage detection system. The proposed method involves creation of a cumulative probability distribution of maximum strain values which provides a representation of the “bridge signature”. We captured truck events due to daily traffic strain measurements from the Powder Mill Bridge in Barre Massachusetts. The absolute maximum strain values from each (heavy) truck event were then used to develop a bridge signature defined on the basis of the shape of the cumulative probability density function of the strain data. Nonparametric statistical methods were introduced for defining the bridge signature and for developing prediction intervals of the signature which can be used to evaluate whether or not significant changes in the bridge signature have occurred. The bootstrap method, a nonparametric statistical method, based on intensive computer based resampling of the observed data, enabled the development of a methodology. This method does not depend on complex statistical theoretical assumptions regarding the sampling properties of estimates of cumulative densities which would be needed for this methodology if a parametric statistical approach were employed.

Three damage scenarios were modeled using a calibrated finite element model of the bridge studied, and in all three cases, the analytical distribution of the damaged structure fell outside of the established prediction intervals for at least one strain gauge, using 1500 truck events. This allows us to conclude that structural damage detection using this method is possible.

In the future, the proposed system could be implemented on newly constructed bridges to assist in bridge inspections, and to provide continuous and operational, long-term monitoring of a bridge's structural health. Future work on this method should include studies of other bridges and creations of bridge signatures using data from a variety of measured operational responses.

Acknowledgments

The authors are grateful for the funding of bridge instrumentation provided by NSF-PFI Grant No. 0650258, and funding for continued system upgrades provided by FHWA LTBP Program (Federal Contract Number DTFH61-08-00005, Sub-award Number 00004397). We would like to thank MassDOT and the Town of Barre for access to the Powder Mill Bridge on Vernon Avenue, and Fay Spofford & Thorndike Inc. for sharing with us the design drawings and calculations. Additionally, we wish to thank Geocomp Corporation for providing and assisting with the installation of the onsite data acquisition system, and for continued technical support. Finally, we are thankful the use of the calibrated finite element model of the bridge, which was created by John Phelps.

References

- Alampalli, S., & Lund, R. (2006). "Estimating Fatigue Life of Bridge Components Using Measured Strains." *J. Bridge Eng.*, 11(6), 725–736.
- Cardini, A. J., & DeWolf, J. T. (2009). "Long-Term Structural Health Monitoring of a Multi-Girder Steel Composite Bridge Using Strain Data." *Structural Health Monitoring*, 8(1), 47–58.

- Catbas, F., Zaurin, R., Gul, M., and Gokce, H. (2012). "Sensor Networks, Computer Imaging, and Unit Influence Lines for Structural Health Monitoring: Case Study for Bridge Load Rating." *J. Bridge Eng.*, 17(4), 662–670.
- David, H.A., Order Statistics, John Wiley & Sons, New York, 1981.
- Doebling, S., Farrar, C., Prime, M., and Shevits, D. (1996), Damage Identification and Health Monitoring of Structural and Mechanical Systems from Changes in Their Vibration Characteristics: A Literature Review, *Los Alamos National Laboratory Report*, No. LA-13070-MA, Los Alamos, NM.
- Efron, Bradley & Tibshirani, Robert J. (1993). *An Introduction to the Bootstrap*, Chapman & Hall, New York, NY.
- Farrar, C. R. & Worden, K. (2007). "An Introduction to Structural Health Monitoring." *Phil. Trans. R. Soc.*, 365, 303–315.
- Federal Highway Administration. (2004). "National Bridge Inspections Standards Regulations." www.fhwa.dot.gov/bridge/nbis.cfm
- Federal Highway Administration. (2011). "Traffic Volume Trends." www.fhwa.dot.gov.
- Federal Highway Administration. (2012). "Deficient Bridges by State and Highway System." www.fhwa.dot.gov.
- Lee, Seung-Kyoung. (2012). "Current State of Bridge Deterioration in the US – Part 2." *Materials Performance*, 51(2), 2–7.
- National Institute of Standards and Technology. (2012). "Quantitative Techniques." <http://www.itl.nist.gov/div898/handbook/eda/section3/eda35.htm>
- Ni, Y. Q., Zhou, K. C., Chan, K. C., & Ko, J. M. (2008). "Modal Flexibility Analysis of Cable-Stayed Ting Kau Bridge for Damage Identification." *Computer-Aided Civil and Infrastructure Engineering*, 23(3), 223–236.
- Orcesi, A. D., & Frangopol, D. M. (2010). "Inclusion of Crawl Tests and Long-Term Health Monitoring in Bridge Serviceability Analysis." *J. Bridge Eng.*, 15(3), 312–326.
- Olund, J., & DeWolf, J. (2007). "Passive Structural Health Monitoring of Connecticut's Bridge Infrastructure." *J. Infrastruct. Syst.*, 13(4), 330–339.
- Sanayei, M., Phelps, J., Sipple, J., Bell, E., & Brenner, B. (2012). "Instrumentation, Nondestructive Testing, and Finite-Element Model Updating for Bridge Evaluation Using Strain Measurements." *J. Bridge Eng.*, 17(1), 130–138.
- Sartor, R. R., Culmo, M. P., & DeWolf, J. T. (1999). "Short-Term Strain Monitoring of Bridge Structures." *J. Bridge Eng.*, 4(3), 157–164.
- Scianna, A. M., & Christenson, R. (2009). "Probabilistic Structural Health Monitoring Method Applied to the Bridge Health Monitoring Benchmark Problem," *Transportation Research Record*, 2131, 92–97.
- U.S. Department of Transportation. (2010). *2010 Status of the Nation's Highways, Bridges, and Transit - Conditions and Performance*.

Vogel, Richard M., & Fennessey, Neil M. (1994). "Flow-Duration Curves. I: New Interpretation and Confidence Intervals." *Journal of Water Resources Planning and Management*, (120)4, 485–504.

3. Powder Mill Bridge

3.1 Site and History

The Powder Mill Bridge (PMB) is located at the end of Vernon Avenue by the intersection with MA Route 122 in Barre, Massachusetts. The bridge carries traffic on Vernon Avenue over the Ware River. The PMB experiences a relatively high volume of truck traffic due to its proximity to the Town of Barre Transfer Station for waste management, Figure 3-1.



Figure 3-1. Powder Mill Bridge Location

The PMB was built to replace the old Powder Mill Bridge, Figure 3-2, which had sustained significant structural damage and was demolished prior to construction of the new bridge.



Figure 3-2. Old Powder Mill Bridge

3.2 *New Powder Mill Bridge*

The New PMB was constructed during the first half of 2009, and opened to traffic in September 2009. The bridge was designed by Fay, Spofford, and Thorndike, and was constructed by ET&L Corporation.

PMB is a three-span continuous slab on steel girder bridge. The main span is 23.5 meters (77.1 feet) in length and Spans 1 and 3 are each 11.75 meters (38.6 feet). Spans 1 and 2 are 12.715 meters (41.72 feet) wide; the width of Span 3 varies along its length.

The bridge carries two lanes of traffic in opposite directions, and carries a sidewalk on the east side. The bridge also carries a 200mm (7.87 inch) town water pipe across the river.

The PMB is comprised of six steel girders, each of which has a single splice, and a continuous concrete deck 200mm (7.87 inches) thick. The girders are spaced at 2.25 meters (7.38 feet), and are stiffened laterally with steel diaphragms.

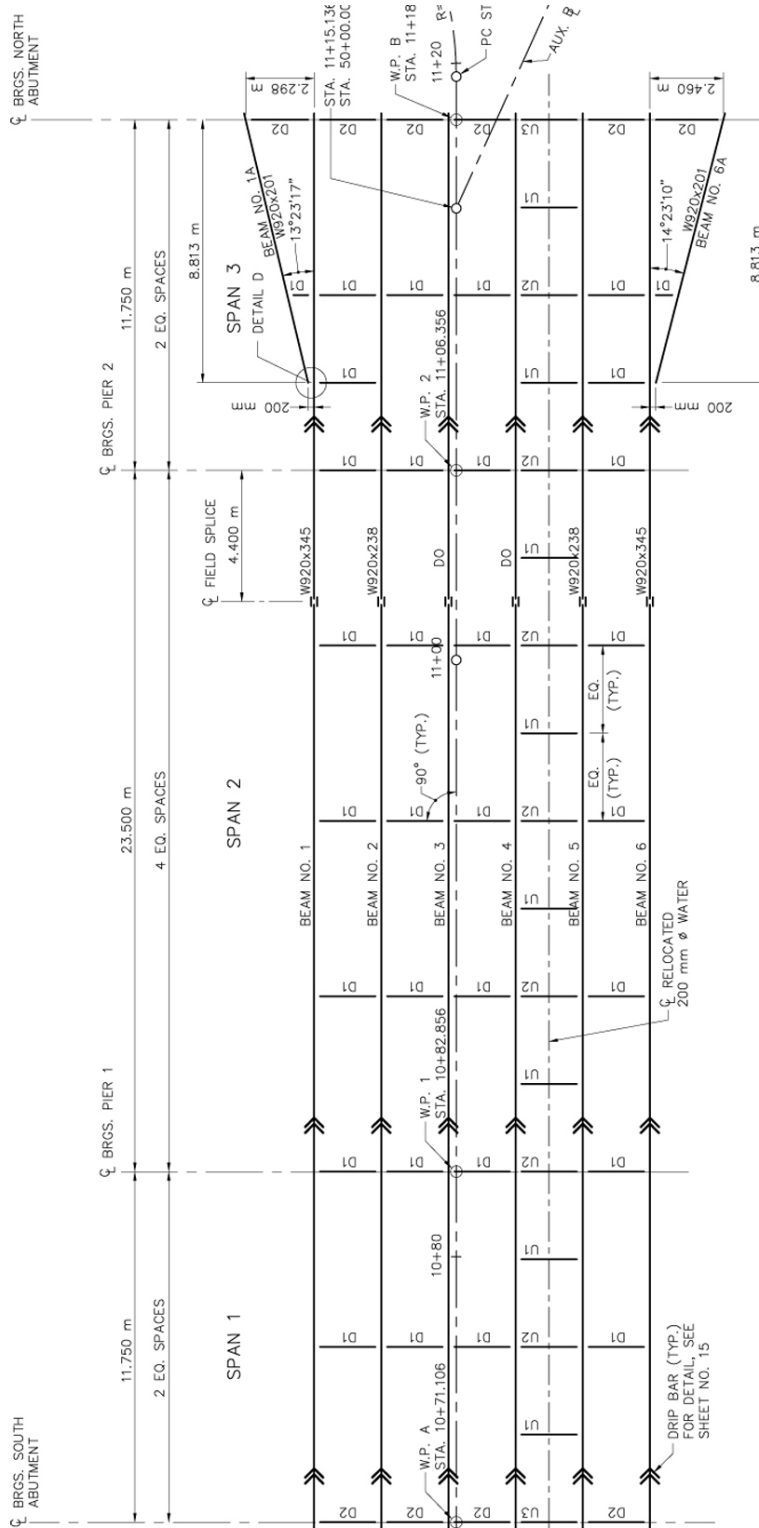


Figure 3-3. Plan View of Powder Mill Bridge

3.3 Instrumentation of Powder Mill Bridge

Instrumentation of the Powder Mill Bridge began in June 2009 and was completed in October 2009. A variety of sensors were installed; details of sensor types, quantities, and locations are shown in Tables 3-1, 3-2, and 3-3, and Figure 3-5.

Table 3-1. PMB Sensor Inventory

Quantity	Sensor Type
100	Strain Gauge
36	Steel Temperature Sensor
36	Concrete Temperature Sensor
16	Tiltmeter
16	Accelerometer
4	Ambient Temperature Sensor
2	Dummy Gauge
2	Pressure Plate

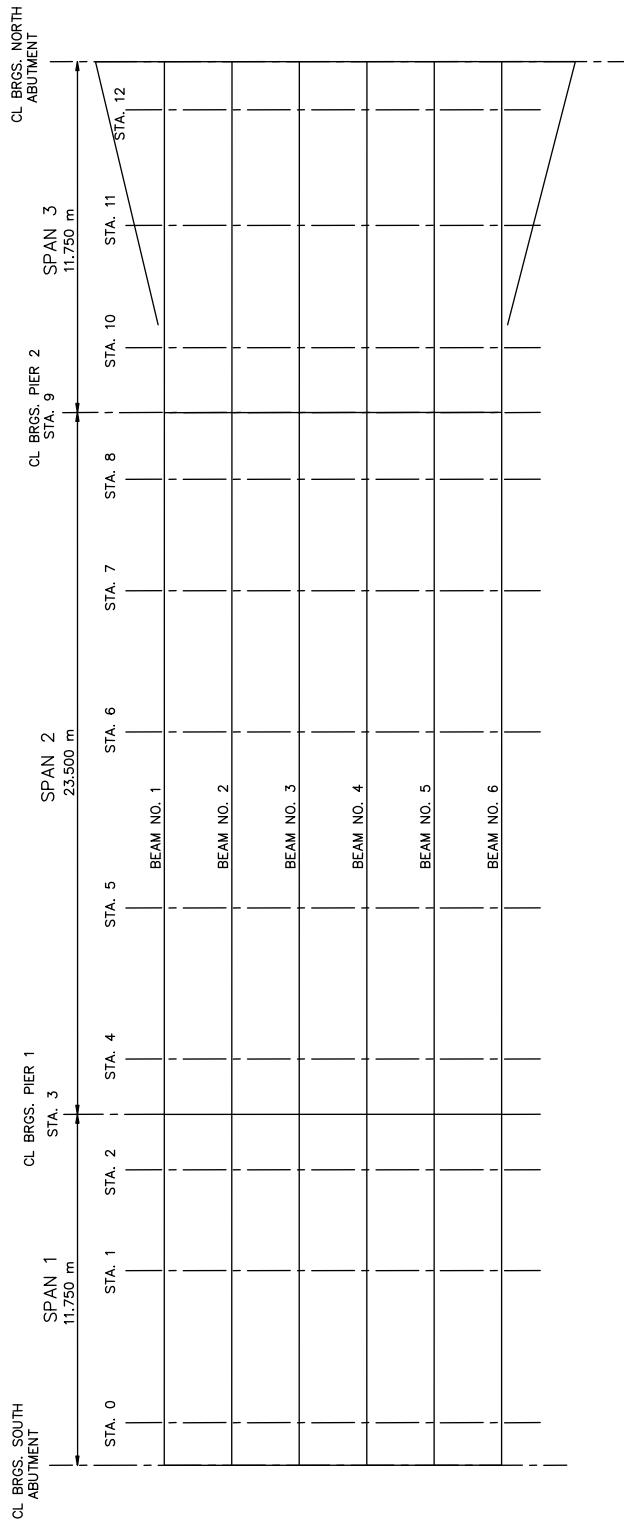


Figure 3-5. PMB Sensor Station Locations

Table 3-2. PMB Instrumentation Schedule, Stations 0 – 6

		Station 0	Station 1	Station 2	Station 3	Station 4	Station 5	Station 6
Girder 1	<i>Deck</i>			2 Concrete Temperature				2 Concrete Temperature
	<i>Top Flange</i>			1 Strain 1 Temperature		1 Strain		1 Strain 1 Temperature
	<i>Web</i>		1 Accel		1 Tiltmeter			1 Accel
	<i>Bottom Flange</i>			1 Strain 1 Temperature		1 Strain		1 Strain 1 Temperature
			1 SWP					1 SWP
Girder 2	<i>Deck</i>			2 Concrete Temperature				2 Concrete Temperature
	<i>Top Flange</i>			2 Strain 1 Temperature		2 Strain		2 Strain 1 Temperature
	<i>Web</i>	1 Tiltmeter	1 Accel		1 Tiltmeter			1 Accel
	<i>Bottom Flange</i>			2 Strain 1 Temperature		2 Strain		2 Strain 1 Temperature
Girder 3	<i>Deck</i>							
	<i>Top Flange</i>			2 Strain 1 Temperature		2 Strain		2 Strain 1 Temperature
	<i>Web</i>		1 Accel					1 Accel
	<i>Bottom Flange</i>			2 Strain 1 Temperature		2 Strain		2 Strain 1 Temperature
Girder 4	<i>Deck</i>			2 Concrete Temperature				2 Concrete Temperature
	<i>Top Flange</i>			2 Strain 1 Temperature		2 Strain		2 Strain 1 Temperature
	<i>Web</i>							
	<i>Bottom Flange</i>			2 Strain 1 Temperature		2 Strain		2 Strain 1 Temperature
Girder 5	<i>Deck</i>							
	<i>Top Flange</i>			2 Strain 1 Temperature		2 Strain		2 Strain 1 Temperature
	<i>Web</i>	1 Tiltmeter			1 Tiltmeter			
	<i>Bottom Flange</i>			2 Strain 1 Temperature		2 Strain		2 Strain 1 Temperature
Girder 6	<i>Deck</i>			2 Concrete Temperature				2 Concrete Temperature
	<i>Top Flange</i>			1 Strain 1 Temperature		1 Strain		1 Strain 1 Temperature
	<i>Web</i>		1 Accel		1 Tiltmeter			1 Accel
	<i>Bottom Flange</i>			1 Strain 1 Temperature		1 Strain		1 Strain 1 Temperature
Abutment		1 Tiltmeter						
Pier Cap					1 Tiltmeter			
1st Bay				2 Concrete Temperature				2 Concrete Temperature

Table 3-3. PMB Instrumentation Schedule, Stations 7 – 12

	Station 7	Station 8	Station 9	Station 10	Station 11	Station 12	Totals
Girder 1				2 Concrete Temperature			6 Concrete Temperature
		1 Strain		1 Strain			5 Strain
				1 Temperature			3 Temperature
	1 Accel		1 Tiltmeter		1 Accel		4 Accel, 2 Tiltmeter
		1 Strain		1 Strain			5 Strain
				1 Temperature			3 Temperature
					1 SWP		3 SWP
Girder 2				2 Concrete Temperature			6 Concrete Temperature
		2 Strain		2 Strain			10 Strain
				1 Temperature			3 Temperature
	1 Accel		1 Tiltmeter		1 Accel	1 Tiltmeter	4 Accel, 4 Tiltmeter
	2 Strain		2 Strain			10 Strain	
			1 Temperature			3 Temperature	
Girder 3				2 Concrete Temperature			6 Concrete Temperature
		2 Strain		2 Strain			10 Strain
	1 Accel			1 Temperature			3 Temperature
	2 Strain		2 Strain		1 Accel		4 Accel
			1 Temperature				10 Strain
							3 Temperature
Girder 4				2 Concrete Temperature			6 Concrete Temperature
		2 Strain		2 Strain			10 Strain
				1 Temperature			3 Temperature
	2 Strain		2 Strain			10 Strain	
			1 Temperature			3 Temperature	
Girder 5				2 Concrete Temperature			6 Concrete Temperature
		2 Strain		2 Strain			10 Strain
				1 Temperature			3 Temperature
			1 Tiltmeter			1 Tiltmeter	4 Tiltmeter
	2 Strain		2 Strain			10 Strain	
			1 Temperature			3 Temperature	
Girder 6				2 Concrete Temperature			6 Concrete Temperature
		1 Strain		1 Strain			5 Strain
				1 Temperature			3 Temperature
	1 Accel		1 Tiltmeter		1 Accel		4 Accel, 2 Tiltmeter
	1 Strain		1 Strain			5 Strain	
			1 Temperature			3 Temperature	
Abutment						1 Tiltmeter	2 Tiltmeter
Pier Cap			1 Tiltmeter				2 Tiltmeter

The research included in this document used only outputs from a subset of the 100 strain gauges installed on the steel girders. The strain gauges were manufactured by Omega Engineering, Inc. (Model KFG-5-120-C1-11L3M3R). The strain gauges were installed on the girders at the fabrication facility of High Steel Structures in Lancaster, PA before the steel was shipped to the construction site. The coating on the weathering steel girders was lightly grinded down to the bare steel, and the surface was sanded and cleaned. The strain gauges were each attached with Loctite glue, covered with silicon, and then the whole arrangement was covered with a weatherproofing aluminum tape, Figure 3-6.



Figure 3-6. Installed Strain Gauge on Powder Mill Bridge

3.4 Data Acquisition System at Powder Mill Bridge

All sensors installed on the Powder Mill Bridge are connected to one Data Acquisition System (DAQ). The system architecture was originally designed by Geocomp Corporation, and employs the use of Geocomp iSite boxes. The sensors are each connected to an iSite box. Each box is capable of supporting eight individual sensors. iSite box information is provided in Table 3-4. Information regarding which sensors are connected to which boxes is provided in Appendix A.

Table 3-4. PMB iSite Box Information

iSite Box Number	IP Address	DB Number	Notes
HS 101	192.168.1.180	DB0088	
HS 102	192.168.1.181	DB0089	
HS 103	192.168.1.182	DB0055	was DB0090 until 9/7/12
HS 104	192.168.1.183	DB0091	
HS 105	192.168.1.184	DB0092	
HS 106	192.168.1.185	DB0093	
HS 107	192.168.1.186	DB0094	
HS 108	192.168.1.187	DB0095	
HS 109	192.168.1.188	DB0096	
HS 110	192.168.1.189	DB0097	
HS 111	192.168.1.190	DB0098	
HS 112	192.168.1.191	DB0099	
HS 113	192.168.1.192	DB0001	
HS 114	192.168.1.193	DB0002	
HS 115	192.168.1.194	DB0003	
HS 116	192.168.1.195	DB0004	
HS 117	192.168.1.196	DB0005	
HS 118	192.168.1.197	DB0006	
HS 119	192.168.1.198	DB0071	was DB0007 until 9/7/12
HS 120	192.168.1.199	DB0008	
V3 Temperature	localhost	-	

All of the iSite boxes on site are connected to a network hub, to which a computer is also connected. Using the computer and Geocomp Corporation's iSiteCC java program, data from the sensors can be collected. The DAQ also includes a router and an IP phone, which allows for remote access to the system. A system architecture schematic is shown in Figure 3-7.

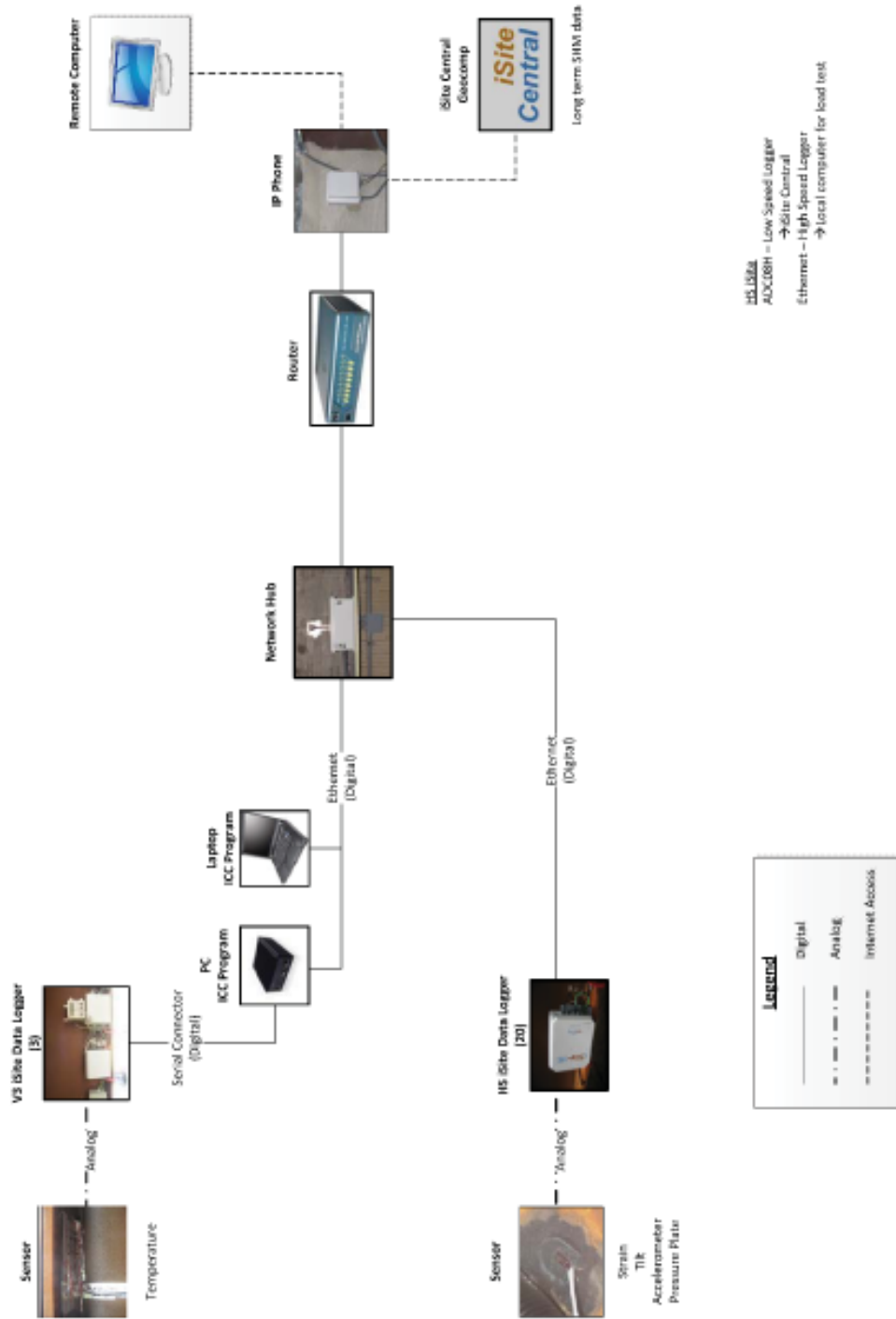


Figure 3-7. PMB DAQ System Architecture Schematic

After completion of the original instrumentation in 2009, modifications to the system have been made. In November 2011, an Uninterrupted Power Supply (UPS) was installed onsite. This addition was made to avoid power surge and short-term power outage issues that were afflicting the system. The UPS was installed in a weather resistant box which was outfitted with both a cooling fan and a heater. The installed UPS and box are shown in Figure 3-8.



Figure 3-8. UPS Installed onsite

The most recent system modification was the addition of a new laptop, which was determined to be necessary for collection of high speed truck event data. The laptop was installed in a weather resistant box, and is connected to the central network hub, which allows for remote access to the laptop, and DAQ management from the laptop. The laptop is also connected to the UPS, and has been programmed so that the UPS can be restarted from the laptop (this can be done remotely). The laptop in its box onsite is shown in Figure 3-9.



Figure 3-9. New Laptop Installed Onsite

4. Long-term Truck Event Data Collection System

4.1 Collection of Truck Events at PMB

In the Spring and Summer of 2012, I designed and installed a software system on the PMB to collect strain data in real time from selected strain gauges from truck events on the bridge. Due to the set up of the DAQ system, truck events could not previously be measured in real time. This means that it was not feasible with the PMB system to record strain data only when trucks are present on the bridge. As a result, my solution was to create a system which collects strain data for 12 hours every day, and then processes the data each night. The system needed to be automatic, efficient, and robust. I used Windows Task Scheduler to automatically run each of the following programs at a specific time each day.

4.2 Automated Collection of Strain Data via iSiteCC Program

The first critical program to the long-term truck event data collection system was the iSiteCC program which was written and provided by Geocomp Corporation. This program allows for automatic collection of sensor values for specified sensors in the system, at specified frequencies. For this research, strain values from all 100 strain gauges were collected for 12 hours each day, at a sampling frequency of 50Hz. Gauge values for each iSite box were saved as individual .csv files, and were written to disk approximately every ten minutes.

4.3 Trigger Program

At the end of each day of data collection, the iSiteCC program has created a folder full of individual .csv files, each of which contains about ten minutes worth of strain data from one iSite box. I wrote a MATLAB program called “Trigger Program” to read in all of the individual files,

put strain values for eighteen selected strain gauges in a large matrix, and then sort through the matrix to identify and save truck events. Saving the truck event data from all 100 strain gauges proved to very computationally intensive, so eighteen gauges distributed across the bridge were chosen as gauges for which the truck event strain data would be saved. Figure 4-1 shows the locations of these gauges. Note that all eighteen gauges are located on the bottom flanges of their respective girders.

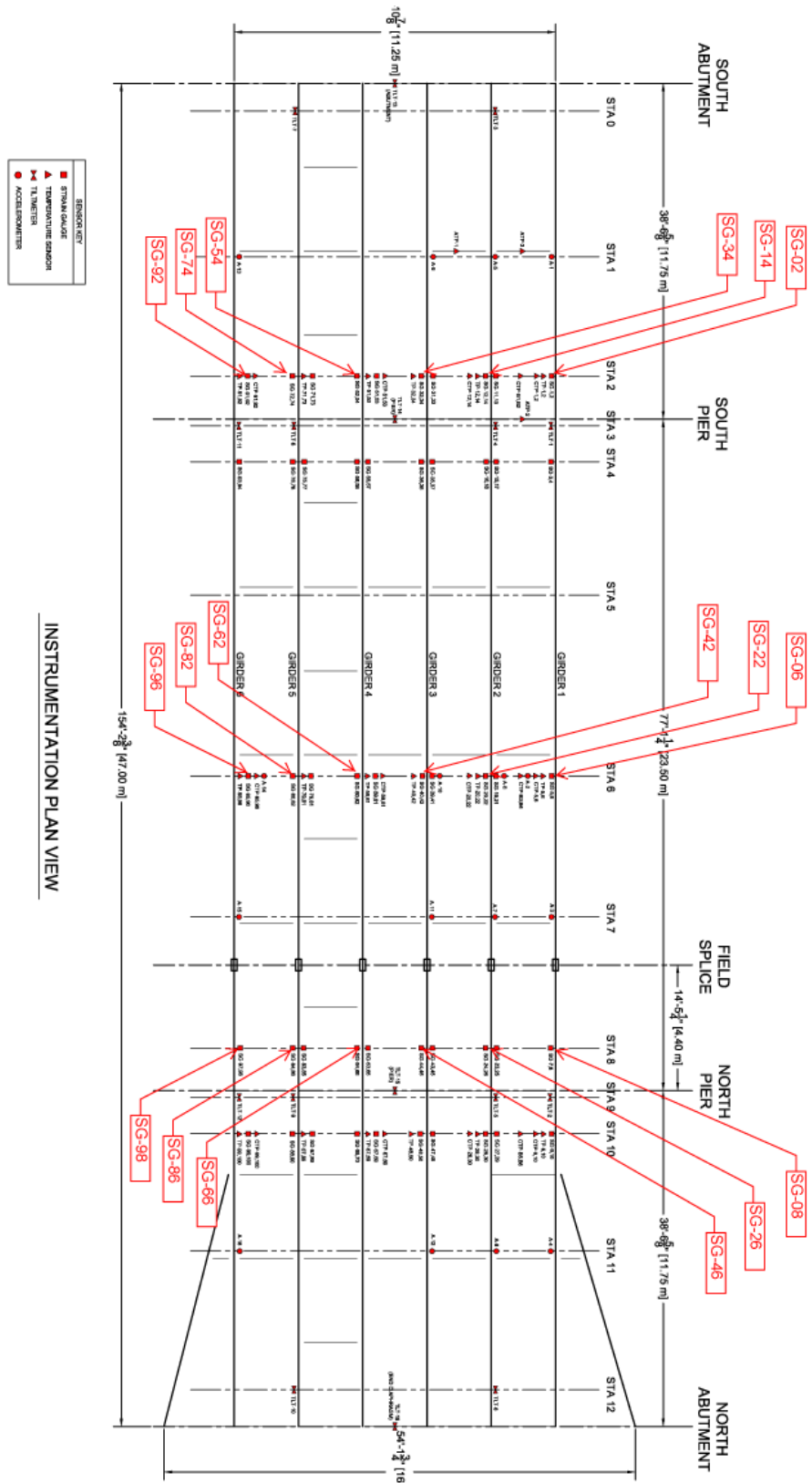


Figure 4-1. Locations of 18 Selected Strain Gauges

The "Trigger Program" uses an algorithm which includes use of the route mean square (RMS) of the strain gauge output values. The program allows the user to input values for a window size (in seconds) and a RMS threshold value (in microstrains). If the RMS value for any of the eighteen gauges is above the threshold value over the defined window size, the program defines that as a truck event. The program then adds user-defined amounts of time on either side of the location where the RMS is above the threshold, and that entire block of time is identified as one truck event. The program then uses ambient data before the event as a zero point, and uses that data (for each gauge) to zero out the truck event data. That is, after zeroing the data, the strain values for all eighteen gauges at the beginning of the event are within a fraction of zero microstrains. This means that the strain data saved is only the strain data due to the truck loading. It does not include strain due to temperature change, snow or ice loading, dead load, or superimposed dead load.

The program has checks to ensure that there was no loading on the bridge during the time period that each zero value is obtained, and that for each truck event, there is strain data from all eighteen sensors. If a good zero value is obtained, and strain data exists for all eighteen sensors during the truck event, the event is saved. Note that a "good zero value" is defined as the average values from the first second of data and the second second of data from each strain gauge having a difference of less than 0.1 microstrains.

Truck events are all saved as MATLAB variables, and contain tables that are nineteen columns wide. The first column contains the time of the reading (this column has a time step of 0.02 seconds between each row). Columns 2 through 19 contain the strain values for each of the eighteen sensors.

All truck event files are written to a specified folder, and can be downloaded via remote access at any time. After a day that truck events have been identified and saved, the .csv raw data file is backed up to an external hard disk onsite, however, the program deletes the original strain data from the hard disk of the laptop.

4.4 Additional Long-term Strain Collection Programs

In addition to the Trigger Program, I wrote another MATLAB program in the system which saves all of the strain values, from all 100 sensors, for the entire 12 hours period each day. This system makes copies of the .csv files from the iSiteCC program, and saves the files on an external hard disk. While these files were not used in the research described here, they are saved and available for future use.

The long-term collection system also includes a program which finds any corrupt or unusable .csv files and deletes them, prior to the Trigger Program starting up.

5. Powder Mill Bridge Calibrated Finite Element Model

5.1 Background on Powder Mill Bridge Calibrated Finite Element Model

A calibrated finite element model (FEM) of the PMB was completed by Tufts University graduate student John Phelps in 2010. The model was created using the PMB design drawings and specifications. The model was then calibrated using strain data collected during a load test on the bridge, which was performed in September 2009. This model was calibrated using strain measurements from a tri-axle dump truck, and can be considered to give reliable strain outputs for model runs using a tri-axle dump truck when the bridge can be assumed to exhibit linear elastic behavior. For more information on the calibrated baseline FEM, refer to Phelps (2010) and Sanayei et al. (2012).

5.2 Undamaged and Damaged Model Truck Runs

As was described in Chapter 2, a model of the tri-axle dump truck was run over undamaged and damaged versions of the calibrated baseline FEM. Damage scenarios are described in Chapter 2.

A summary of strain outputs from the model runs is provided in Table 5-1.

Table 5-1. Absolute Maximum Strains from Calibrated Finite Element Model

	Undamaged	20% Deck Damage Main Span		
	$\mu\epsilon$	$\mu\epsilon$	% Diff	Avg % Diff
SG 34 NB ABS MAX	44.947	46.290	2.99%	3.14%
SG 34 SB ABS MAX	50.016	51.663	3.29%	
SG 42 NB MAX	67.546	68.714	1.73%	1.91%
SG 42 SB MAX	78.545	80.184	2.09%	

	Undamaged	50% Deck Damage Main Span		
	$\mu\epsilon$	$\mu\epsilon$	% Diff	Avg % Diff
SG 34 NB ABS MAX	44.947	49.129	9.30%	10.01%
SG 34 SB ABS MAX	50.016	55.375	10.71%	
SG 42 NB MAX	67.546	71.476	5.82%	6.32%
SG 42 SB MAX	78.545	83.908	6.83%	

	Undamaged	50% Deck Damage Local		
	$\mu\epsilon$	$\mu\epsilon$	% Diff	Avg % Diff
SG 34 NB ABS MAX	44.947	45.05	0.23%	0.51%
SG 34 SB ABS MAX	50.016	50.413	0.79%	
SG 42 NB MAX	67.546	68.254	1.05%	1.72%
SG 42 SB MAX	78.545	80.423	2.39%	

References

- Phelps, J. (2010). "Instrumentation, Nondestructive Testing, and Finite-Element Model Updating for Bridge Evaluation."
- Sanayei, M., Phelps, J., Sipple, J., Bell, E., & Brenner, B. (2012). "Instrumentation, Nondestructive Testing, and Finite-Element Model Updating for Bridge Evaluation Using Strain Measurements." *J. Bridge Eng.*, 17(1), 130–138.

6. Conclusions

6.1 Overall Conclusions

A new methodology of structural health monitoring and structural damage detection has been proposed. This methodology utilizes long-term truck event strain data in the creation of a statistical distribution termed “bridge signature”, which is the expected response of a particular bridge under loading, as measured by different instruments. Distributions of future truck event strain data can be plotted against the bridge signature, and, under certain damage scenarios, the study performed suggests that the distribution from the damaged structure will fall significantly far away from the bridge signature. In this case, it can be concluded that structural damage has likely occurred.

The proposed methodology requires only strain outputs from truck events over a substantially long period of time. It can be considered an operational monitoring system, as the bridge inputs (truck weight, weight distribution, load path, etc.) are not needed.

While the method cannot locate or quantify damage, it provides a reasonable solution for passive monitoring of structural deck damage identification. The system could be implemented as complementary to mandatory bridge inspections by engineers, and should be considered as providing engineers with additional information about the structural health of a bridge, rather than an all-inclusive method of structural damage identification, damage location, and damage quantification. Statistical Bridge Signatures can be used for triggering visual inspections and use of other methods of local and global health monitoring.

6.2 *Future Work*

While the results presented here suggest that the proposed method has noteworthy potential, there are several areas that should be studied further.

First, a better understanding of how bridge outputs change under different damage scenarios needs to be gained. This study presents only results from deck damage scenarios; other damage scenarios should be studied, and the typical changes in the absolute maximum strain distributions should be established.

Second, a study should be done on what other data types could be used with the proposed method. This study used only strain outputs from the steel girders, but this method could potentially be implemented with accelerations, tilts, displacements, or other data types.

Third, a study should be performed on where sensors should be installed on a bridge to optimize damage detection potential (with respect to the method proposed here) for a variety of damage scenarios.

Fourth, how best to synthesize data collected from different sensors and different sensors types should be considered. This study included signature distributions from (2) strain gauges. If new distributions fall outside of the established 95% prediction intervals for both gauges that may provide more certainty that structural damage has in fact occurred.

Fifth, systems need to be established for how to include the use of the proposed method in the typical bridge inspection process.

Finally, and most critically, it must be noted that this method was studied for one specific bridge, with loading from one specific vehicle type. Different bridge types and different vehicle types must be studied to validate this method for more general application.

Appendix A: Powder Mill Bridge Supplemental Information

Table A-1. Sensor Information for 18 Selected Strain Gauges on PMB

	Name	Name Description	Type	Type Description	Manufacturer	Units: Feet			Inches		
						X Location (Longitudinal)	Y Location (Transverse)	Z Location (Vertical)	X Location (Longitudinal)	Y Location (Transverse)	Z Location (Vertical)
2	SG_2_G1_BF_0911	Strain Gage 2, Girder 1, Bot. Flange, 0.911	KFG-5-350-C1-11L3M3R	3-wire uniaxial Strain Gauge, 350 Ohm	Omega	34.3663878	38.88974667	-41.2555	34.3663878	38.88974667	-41.2555
6	SG_6_G1_BF_0912	Strain Gage 6, Girder 1, Bot. Flange, 0.912	KFG-5-350-C1-11L3M3R	3-wire uniaxial Strain Gauge, 350 Ohm	Omega	80.30052493	38.894955	-41.2555	80.30052493	38.894955	-41.2555
8	SG_8_G1_BF_0912	Strain Gage 8, Girder 1, Bot. Flange, 0.912	KFG-5-350-C1-11L3M3R	3-wire uniaxial Strain Gauge, 350 Ohm	Omega	111.576345	39.06141816	-40.7055	111.576345	39.06141816	-40.7055
14	SG_14_G2_BF_0911	Strain Gage 14, Girder 2, Bot. Flange, 0.911	KFG-5-350-C1-11L3M3R	3-wire uniaxial Strain Gauge, 350 Ohm	Omega	34.3663878	31.68633833	-40.7055	34.3663878	31.68633833	-40.7055
22	SG_22_G2_BF_0912	Strain Gage 22, Girder 2, Bot. Flange, 0.912	KFG-5-350-C1-11L3M3R	3-wire uniaxial Strain Gauge, 350 Ohm	Omega	80.29010827	31.68633833	-40.7055	80.29010827	31.68633833	-40.7055
26	SG_26_G2_BF_0912	Strain Gage 26, Girder 2, Bot. Flange, 0.912	KFG-5-350-C1-11L3M3R	3-wire uniaxial Strain Gauge, 350 Ohm	Omega	111.576345	31.68633833	-40.7055	111.576345	31.68633833	-40.7055
34	SG_34_G3_BF_0911	Strain Gage 34, Girder 3, Bot. Flange, 0.911	KFG-5-350-C1-11L3M3R	3-wire uniaxial Strain Gauge, 350 Ohm	Omega	34.36617946	24.32196333	-38.9345	34.36617946	24.32196333	-38.9345
42	SG_42_G3_BF_0912	Strain Gage 42, Girder 3, Bot. Flange, 0.912	KFG-5-350-C1-11L3M3R	3-wire uniaxial Strain Gauge, 350 Ohm	Omega	80.30052493	24.30633833	-38.9345	80.30052493	24.30633833	-38.9345
46	SG_46_G3_BF_0912	Strain Gage 46, Girder 3, Bot. Flange, 0.912	KFG-5-350-C1-11L3M3R	3-wire uniaxial Strain Gauge, 350 Ohm	Omega	111.5280512	24.30633833	-38.9345	111.5280512	24.30633833	-38.9345
54	SG_54_G4_BF_0911	Strain Gage 54, Girder 4, Bot. Flange, 0.911	KFG-5-350-C1-11L3M3R	3-wire uniaxial Strain Gauge, 350 Ohm	Omega	34.3663878	16.936755	-40.2936	34.3663878	16.936755	-40.2936
62	SG_62_G4_BF_0912	Strain Gage 62, Girder 4, Bot. Flange, 0.912	KFG-5-350-C1-11L3M3R	3-wire uniaxial Strain Gauge, 350 Ohm	Omega	80.32195827	16.92633833	-40.2936	80.32195827	16.92633833	-40.2936
66	SG_66_G4_BF_0912	Strain Gage 66, Girder 4, Bot. Flange, 0.912	KFG-5-350-C1-11L3M3R	3-wire uniaxial Strain Gauge, 350 Ohm	Omega	111.576345	16.91592275	-40.2936	111.576345	16.91592275	-40.2936
74	SG_74_G5_BF_0911	Strain Gage 74, Girder 5, Bot. Flange, 0.911	KFG-5-350-C1-11L3M3R	3-wire uniaxial Strain Gauge, 350 Ohm	Omega	34.3663878	9.556755	-42.065	34.3663878	9.556755	-42.065
82	SG_82_G5_BF_0912	Strain Gage 82, Girder 5, Bot. Flange, 0.912	KFG-5-350-C1-11L3M3R	3-wire uniaxial Strain Gauge, 350 Ohm	Omega	80.30052493	9.54633833	-42.065	80.30052493	9.54633833	-42.065
86	SG_86_G5_BF_0912	Strain Gage 86, Girder 5, Bot. Flange, 0.912	KFG-5-350-C1-11L3M3R	3-wire uniaxial Strain Gauge, 350 Ohm	Omega	111.576345	9.541131033	-42.065	111.576345	9.541131033	-42.065
92	SG_92_G6_BF_0911	Strain Gage 92, Girder 6, Bot. Flange, 0.911	KFG-5-350-C1-11L3M3R	3-wire uniaxial Strain Gauge, 350 Ohm	Omega	34.3663878	1.97933	-44.386	34.3663878	1.97933	-44.386
96	SG_96_G6_BF_0912	Strain Gage 96, Girder 6, Bot. Flange, 0.912	KFG-5-350-C1-11L3M3R	3-wire uniaxial Strain Gauge, 350 Ohm	Omega	80.3109416	1.989746667	-44.386	80.3109416	1.989746667	-44.386
98	SG_98_G6_BF_0912	Strain Gage 98, Girder 6, Bot. Flange, 0.912	KFG-5-350-C1-11L3M3R	3-wire uniaxial Strain Gauge, 350 Ohm	Omega	111.5332595	2.16662649	-44.386	111.5332595	2.16662649	-44.386

Table A-2. Data Acquisition System Information for 18 Selected Strain Gauges

PMB SENSOR LIST
CWF 06.05.12

STRAIN GAUGE	STATION	GIRDER	ISITE	ADDRESS	CHANNEL #
2	2	1	113	DB0001	2
6	6	1	113	DB0001	6
8	8	1	113	DB0001	8
14	2	2	111	DB0098	2
22	6	2	111	DB0098	6
26	8	2	110	DB0097	2
34	2	3	109	DB0096	2
42	6	3	108	DB0095	2
46	8	3	108	DB0095	6
54	2	4	107	DB0094	6
62	6	4	106	DB0093	6
66	8	4	105	DB0092	2
74	2	5	104	DB0091	2
82	6	5	103	DB0090	2
86	8	5	103	DB0090	6
92	2	6	102	DB0089	4
96	6	6	102	DB0089	8
98	8	6	101	DB0088	2